Published OnlineFirst February 3, 2009; DOI: 10.1158/0008-5472.CAN-08-3198

Research Article

Human Renal Cancer Cells Express a Novel Membrane-Bound Interleukin-15 that Induces, in Response to the Soluble Interleukin-15 Receptor α Chain, Epithelial-to-Mesenchymal Transition

Krystel Khawam,[1] Julien Giron-Michel,[1] Yanhong Gu,[1] Aurélie Perier,[3] Massimo Giuliani,[1] Anne Caignard,[3] Aurore Devocelle,[1] Silvano Ferrini,[4] Marina Fabbi,[4] Bernard Charpentier,[1] Andreas Ludwig,[5] Salem Chouaib,[2] Bruno Azzarone,[1] and Pierre Eid[1]

[1]Institut National de la Sante et de la Recherche Medicale UMR 542, Université de Paris-Sud, Hôpital Paul Brousse; [2]Institut National de la Sante et de la Recherche Medicale UMR 753, Université de Paris-Sud, Institut Gustave Roussy, Villejuif, France; [3]Institut National de la Sante et de la Recherche Medicale U 567, Institut Cochin, Paris, France; [4]Laboratory of Immunotherapy, Istituto Nazionale per la Ricerca sul Cancro, Genova, Italy; and [5]Institute for Pharmacology, RWTH Aachen University, Aachen, Germany

Abstract

Although interleukin-15 (IL-15) is a powerful immunomodulatory factor that has been proposed for cancer immunotherapy, its intratumoral expression may be correlated with tumor progression and/or poor clinical outcome. Therefore, neoplasias potentially sensitive to immunotherapy should be checked for their IL-15 expression and function before choosing immunotherapy protocols. Primary human renal cancer cells (RCC) express a novel form of membrane-bound IL-15 (mb-IL-15), which displays three major original properties: (*a*) It is expressed as a functional membrane homodimer of 27 kDa, (*b*) it is shed in the extracellular environment by the metalloproteases ADAM17 and ADAM10, and (*c*) its stimulation by soluble IL-15 receptor α (s-IL-15Rα) chain triggers a complex reverse signal (mitogen-activated protein kinases, FAK, pMLC) necessary and sufficient to ~induce epithelial-mesenchymal transdifferentiation (EMT), a crucial process in tumor progression whose induction is unprecedented for IL-15. In these cells, complete EMT is characterized by a dynamic reorganization of the cytoskeleton with the subsequent generation of a mesenchymal/contractile phenotype (α-SMA and vimentin networks) and the loss of the epithelial markers E-cadherin and ZO-1. The retrosignaling functions are, however, hindered through an unprecedented cytokine/receptor interaction of mb-IL-15 with membrane-associated IL-15Rα subunit that tunes its signaling potential competing with low concentrations of the s-IL-15Rα chain. Thus, human RCC express an IL-15/IL-15R system, which displays unique biochemical and functional properties that seem to be directly involved in renal tumoral progression. [Cancer Res 2009;69(4):1561–9]

Introduction

Interleukin-15 (IL-15) is a proinflammatory cytokine that plays an important role in both the innate and adaptive immune system. IL-15 promotes the activation of neutrophils and macrophages and is critical to dendritic cell function. In addition, IL-15 is essential to the development, homeostasis, function, and survival of natural killer (NK) cells, NK T cells, and memory CD8+ T cells. Based on these properties, IL-15 has been proposed as a useful cytokine for immunotherapy (1).

Indeed, in preclinical models, IL-15 displays antitumor activity mainly mediated by CD8+ T cells and NK cells (2–4). However, in humans, recent clinical studies reported a correlation between high intratumoral IL-15 concentrations and poor clinical outcome in patients with lung or head and neck cancers (5, 6). Moreover, IL-15 production by human melanoma, colon cancer, or prostate cancer cells contributes to the progression of the disease (7–12).

IL-15 is a 14-kDa cytokine that belongs to the four-helix bundle cytokine family and was first characterized by its ability to substitute IL-2. Indeed, IL-15 shares with IL-2 the IL-2 receptor (IL-2R) β and γ chains but has a unique private α chain (IL-15Rα) that is responsible for high-affinity binding and signal transduction (13). In addition, IL-15Rα may be secreted as a functional soluble molecule (s-IL-15Rα) that behaves as an agonist or antagonist for IL-15, depending on its cleavage mechanism certainly in mouse and probably in human (14–16).

Three different functional forms of IL-15 have been identified: (*a*) the soluble cytokine secreted by accessory cells (at pg/mL) that activates cells expressing high-affinity IL-15R (1), (*b*) the hyper IL-15 (s-IL-15/IL-15Rα complex) 100-fold more efficient than the noncomplexed soluble cytokine (17, 18), and (*c*) the membrane-bound forms (mb-IL-15) considered as the dominant physiologic forms of the cytokine (17, 19, 20). Thus, a mb-IL-15 anchored through IL-15Rα, which activates by transpresentation of bystander cells, has been described. This mechanism is essential for lymphoid homeostasis, both in mice and man. In addition, human cells display two other forms of mb-IL-15. The first one, anchored at the surface of spleen stromal cells through the IL-15Rαβγc complex, is able to induce NK differentiation (17). The other one is an IL-15R–independent mb-IL-15 that can function as a receptor and participate in reverse signaling and/or act in a juxtacrine fashion (19).

IL-15 has been involved in renal inflammatory pathologies in mice and human but with contrasting conclusion between the two species (21, 22). Furthermore, cytosolic and nonsecreted IL-15

Note: Supplementary data for this article are available at Cancer Research Online (http://cancerres.aacrjournals.org/).

K. Khawam, J. Giron-Michel, and Y. Gu contributed equally to this article.

Present address for Y. Gu: Department of Clinical Oncology, Nanjing Medical University, China.

Requests for reprints: Azzarone Bruno, Institut National de la Sante et de la Recherche Medicale, UMR 542, Bâtiment Lavoisier, Hôpital Paul Brousse, 14, Avenue Paul Vaillant Couturier, 94807, Villejuif Cedex, France. Phone: 33-0145595343; Fax: 33-0145595344; E-mail: bazzarone@hotmail.com.

doi:10.1158/0008-5472.CAN-08-3198

Published OnlineFirst February 3, 2009; DOI: 10.1158/0008-5472.CAN-08-3198

protein was reported in renal cell carcinoma (RCC; ref. 23), whereas we have recently reported that human RCC express a mb-IL-15 form that is able to protect NK cells from apoptosis (24).

To determine the role of IL-15 in human renal cancer progression, we here investigated the expression and function of the IL-15/IL-15R complex in RCC. Our data show that RCCs express a functional IL-15/IL-15R system characterized by unique properties apparently "specific" to RCCs that finely tune and shape the functions of this cytokine. Indeed, RCCs express a novel mb-IL-15 form, likely expressed as a homodimer of 27 kDa (mb-IL-15), sensitive to metalloproteases. In response to a soluble specific ligand (s-IL-15Rα), tumor IL-15 activates a reverse signal that induces epithelial-mesenchymal transdifferentiation (EMT). These signaling functions are, however, modulated through the interaction of mb-IL-15 with membrane-associated IL-15Rα subunit present in the same cell, which tunes its signaling potential.

Materials and Methods

Antibodies, cytokines, and reagents. Antibodies against IL-15 [monoclonal antibody (mAb) L-20], extracellular signal-regulated kinase (ERK), stress-activated protein kinase (SAPK)/c-Jun NH_2 kinase (JNK), FAK (C-20), phosphorylated FAK, p38, E-cadherin (HB-108), pMLC (sc-12896), vimentin (sc-32322), α-tubulin (sc-8035), ZO-1, and IL-15Rα (sc-9172) were purchased from Santa Cruz Biotechnology. pp38, pERK, pSAPK/JNK antibodies were purchased from Cell Signaling. Anti-IL-15-phycoerythrin (mAb247-PE), anti-IL-15Rα (mAb147), rhuIL-15 Rα/Fc chimera soluble (s-IL-15Rα) chain, and transforming growth factor-β (TGF-β) were purchased from R&D Systems Europe Ltd. mAb anti-CD122/IL-2Rβ (TMβ1) and anti-CD132/IL-2Rγ/γc (4G2) antibodies were purchased from BD Pharmingen. Bovine serum albumin (BSA), phosphatidylinositol-specific phospholipase C (PI-PLC), 1-10-phenantrolin (Phen), and iodoacetamide were purchased from Sigma-Aldrich. Rabbit anti-α-SMA antibody was purchased from Epitomics. Horseradish peroxidase–conjugated rabbit anti-goat, rabbit anti-mouse, goat anti-mouse, and goat anti-rabbit secondary antibodies (Amersham Biosciences) were used. Fluorescent secondary antibodies, goat anti-mouse FITC and goat anti-rabbit FITC (Jackson), were used. Antibodies against CD59, ADAM10, and ADAM17 and the recombinant human IL-15 (rhIL-15) were from ImmunoTools.

Cell culture. Primary tumor (RCC5-T), normal renal (RCC5-N), and primary metastatic cells (RCC5-M) from the same patients, and primary tumor cells (RCC7) were obtained by enzymatic digestion of renal tumor as described previously (25). RCC primary cultures, ACHN, HIEG (metastasis), A704, Caki-2 renal cell lines, HK2 (human embryonic epithelial renal cells immortalized by papilloma virus), and small cell lung carcinoma N592 were maintained in DMEM (Life Technologies) supplemented with 10% FCS, 1% MEM sodium pyruvate (Life Technologies), and 1% penicillin/streptomycin (Life Technologies). Erythroleukemia cell line TF1β and megakaryoblastic leukemic cell line UT7 were maintained in RPMI 1640 (Life Technologies) supplemented with 10% FCS, 1% L-glutamine (Life Technologies), 1% penicillin/streptomycin, 5 ng/mL granulocyte macrophage colony-stimulating factor (GM-CSF; R&D System), and 0.5 mg/mL G418 (Life Technologies). Peripheral blood lymphocytes (PBL) and peripheral blood monocytes were prepared as described previously (17).

Stimulation and treatments. In some experiments, acidic shock was performed, incubating cells in ice-cold 0.1 mol/L sodium acetate (pH 4.0) for 15 min at 4°C, whereas PI-PLC treatment was realized with 5 units/mL for 1 h at 37°C. In other experiments, RCCs were stimulated with phorbol 12-myristate 13-acetate (PMA; 200 ng/mL) or with orthopervanadate (PVN; 200 μmol/L) in FCS-free medium for 3 h at 37°C. Competition experiments were performed by incubating the cells with a broad-spectrum metalloprotease inhibitor Phen (2 mmol/L) or potent inhibitors for the metalloproteases ADAM10 (GI254023X) and ADAM17 (GW280264X) used at 10 μmol/L, as previously described (26). For biochemical analysis, supernatants were collected soon after treatments concentrated 10-fold using Amicon Ultra-4 Ultracel-10K regenerated cellulose 10,000 MWCO (Millipore).

Flow cytometry analysis. Flow cytometry cell surface analysis was performed as previously described (22). For each sample, 10,000 cells were acquired for data analysis using FACSCalibur and analyzed with CellQuest software (BD Biosciences).

Reverse transcription–PCR analysis. Total RNA was isolated by the NucleoSpin RNA II kit (Macherey-Nagel) according to the manufacturer's instructions. Total RNA (1 μg) was then subjected to the SuperScript II reverse transcriptase (Invitrogen) in 20 μL. cDNA (2 μL) was separately amplified in 25 μL, with 2.5 IU Taq polymerase (Genecraft), in the presence of 1 μmol/L of the primers specific for IL-15, IL-15Rα, or the γ_c, and for the housekeeping gene β-actin. The amplifications were carried out in a PCR Sprint thermal cycler (Hybaid) for 35 or 25 cycles for β-actin (15 s at 94°C, 15 s at 60°C, 30 s at 72°C) with a final extension at 72°C for 5 min. PCR products (10 μL) were then analyzed in 1% to 2% agarose gel containing ethidium bromide. Specific primers are detailed in Supplementary Table S1.

Plasma membrane and cytosolic fractions separation. Cells were washed twice with ice-cold PBS and subsequently homogenized with glass Dounce homogenizer (10 mmol/L Tris, 0.25 mmol/L sucrose, 2 mmol/L EDTA, 2 mmol/L protease inhibitors). The homogenate was first centrifuged at 2,500 × *g* for 30 min at 4°C to pellet nuclei and whole cells and then at 100,000 × *g* for 30 min at 4°C (cytosolic fraction). The pellet containing the plasma membrane was resuspended in 10 mmol/L Tris (pH 7.4), 150 mmol/L NaCl, 2 mmol/L $CaCl_2$, 2 mmol/L $MgCl_2$, 1% digitonin, and 2 mmol/L protease inhibitors. The detergent-insoluble materials were removed by centrifugation for 15 min at 13,000 rpm at 4°C (plasma membrane fraction). Immunoprecipitations were performed on both plasma membrane and cytosolic fractions (17).

Immunoprecipitation and immunoblotting. For immunoprecipitation and Western blotting, cells were lysed in 1% digitonin cell extraction buffer [1 mmol/L EDTA, 150 mmol/L NaCl, 20 mmol/L Tris (pH 8.0), and 10% glycerol] and protease inhibitor cocktail tablets (complete, Roche). For immunoprecipitation, lysates and plasma membrane fraction were first precleared with the protein G-sepharose (GE Healthcare Bioscience AB) then incubated overnight at 4°C in 0.1% digitonin buffer with 5 μg/mL of antibodies against IL-15 bound to protein G-sepharose or antigoat IgG bound to protein G-sepharose as control. After washing, the immunocomplexes were boiled 5 min in SDS sample buffer and analyzed in 15% SDS-PAGE. The resolved proteins were transferred onto polyvinylidene difluoride (PVDF) membranes (Immobilon). Blots were blocked for 2 h in PBS with 0.1% Tween 20 and 5% nonfat milk. Immunoreactive proteins were detected using the Super Signal West Pico and West Fempto kits (Pierce). In some experiments, DTT was added at 20 mmol/L to PVN-treated RCC7 cell supernatant. After 20 min, at 60°C, iodoacetamide was added at 100 mmol/L and incubated in the dark for 20 min at 20°C. SDS sample buffer was subsequently added, and proteins were then separated by 15% SDS-PAGE without using any reducing agent. IL-15 was visualized by Western blot analysis.

Phosphospecific Western blotting. For signal transduction, cells were washed twice with Dulbecco's PBS and serum-starved overnight. RCCs were then stimulated with s-IL-15Rα (1–500 ng/mL) for periods ranging between 15 min and 4 h. Activation was interrupted by adding two to three volumes of ice-cold PBS. Cell pellets were lysed for 30 min on ice in 1% Triton X-100, 20 mmol/L Tris-HCl (pH 7.4), 137 mmol/L NaCl, 2 mmol/L EDTA, 2 mmol/L sodium pyrophoshate, and 10% glycerol in the presence of the phosphatases inhibitors (25 mmol/L β-glycerophophate and 1 mmol/L sodium orthovanadate) and the protease inhibitor cocktail tablets. The detergent-insoluble material was removed by centrifugation at 12,000 rpm for 15 min at 4°C. The resolved proteins were transferred onto PVDF membranes and processed as described previously (27).

Two-dimensional gel electrophoresis. The IL-15 concentrated from serum-free RCC7 cell medium after pervanadate treatment (2×10^7 cells) was equilibrated in 200 μL of 40 mmol/L Tris base, 8 mol/L urea, 2 mol/L thiourea, 1.2% CHAPS (w/v), 0.4% ASB-14 (w/v), 20 mmol/L DTT, 0.5% IPG buffer 3-11 NL, and 0.002% bromophenol blue solution. The isoelectric focusing step was performed on Immobiline Drystrip pH 3-11 NL (11 cm)

Published OnlineFirst February 3, 2009; DOI: 10.1158/0008-5472.CAN-08-3198

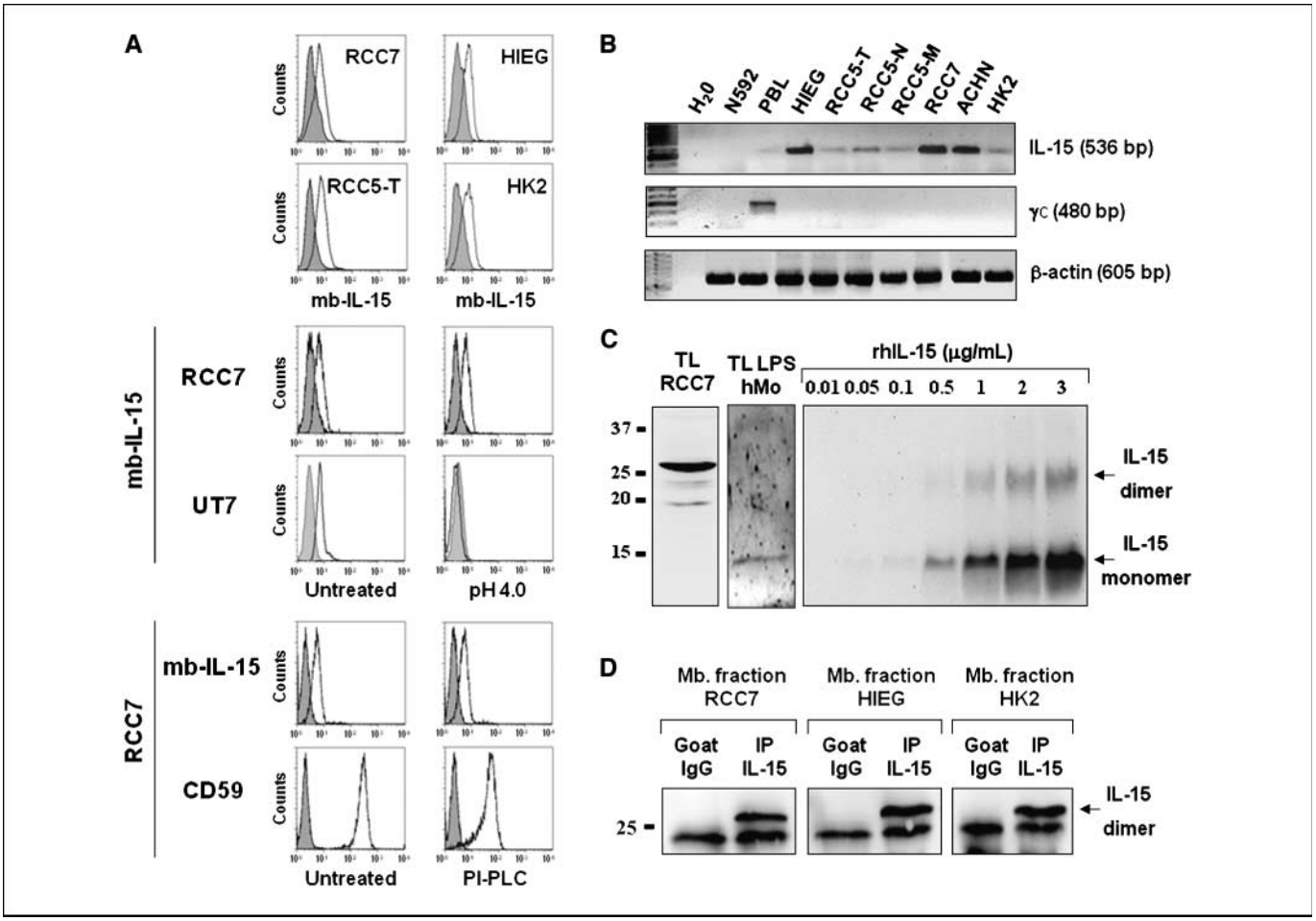

Figure 1. mb-IL-15 characterization in human RCC. *A, top,* detection in human primary (*RCC5-T* and *RCC7*), metastatic (*HIEG*), and virus-transformed (*HK2*) RCC of mb-IL-15 expression by flow cytometry (mAb 247-PE, *open peaks*). *Middle,* sensitivity of mb-IL-15 (*open peaks*) to acidic shock (*pH 4.0*) was evaluated by fluorescence-activated cell sorting analysis in RCC7 cells. The human erythroleukemic UT7 cells were used as control of expression of the mb-IL-15 form sensitive to this treatment. *Bottom,* the possibility that in RCC mb-IL-15 is a GPI-linked protein was studied by flow cytometry investigating the sensitivity of mb-IL-15 (*open peaks*) to PI-PLC. CD59, a GPI-anchored protein, is used as positive control of PI-PLC cleavage. Isotype-matched antibodies were used as control (*shaded peaks*). Representative of three independent experiments. *B,* detection of the IL-15 and γc chain transcripts in human RCC by RT-PCR. The human microcitoma cell line cell N592 was used as negative control, whereas human PBLs were used as positive control for γc chain expression. Amplification of the same cDNAs with β-actin specific primers is shown as loading control. Representative of three independent experiments. *C,* Western blotting with an anti-IL-15 goat antibody L-20, on total lysate (*TL*) of RCC7 cells, of lipopolysaccharide-stimulated human monocytes, and on increasing concentrations (0.01–3 μg/mL) of the recombinant human IL-15. Representative of three different experiments. *D,* immunoprecipitation with an anti-IL-15 goat antibody L-20 on the plasma membrane fraction (*Mb. fraction*) of RCC7, HIEG, and HK2 cell lines. The membrane was subsequently probed with the same L-20 antibody. A single 27-kDa specific band was detected, whereas the isotype control (*Goat IgG*) did not detect any band. These results are representative of three different experiments.

using an IPGphor (GE Healthcare Amersham) according to the manufacturer's instructions. The second dimension was performed on a 15% SDS-PAGE. IL-15 was revealed by immunoblot as described above.

Induction of EMT of RCC. Exponentially growing RCC were incubated in normal growth medium containing 5 ng/mL TGF-β or 100 ng/mL of s-IL-15Rα on Lab-Tek chamber slide system 177445 (Nalge Nunc International) for 6 d. Subsequently, cells were washed twice with PBS and then fixed in 4% paraformaldehyde for 30 min on ice. Before staining with anti-α-SMA, anti-ZO-1, or anti-vimentin antibodies, RCC were permeabilized with 0.1% TX-100 for 5 min on ice, then saturated in 0.1% BSA for 30 min on ice. E-cadherin staining was performed without permeabilization. As secondary antibodies, FITC-conjugated goat anti-mouse subclasses IgG1 were used and 4′,6-diamidino-2-phenylindole was added to visualize the nucleus. The cells were washed thrice with 0.1% BSA and then with PBS. The chamber slides were removed, and the samples were mounted in Mowiol by adding a glass coverslip. All samples were observed with an oil immersion objective (Plan-Neofluar 40×/1.3, Ph3; Zeiss) through an Axiophot Zeiss microscope (Zeiss). Digital images were taken with a digital color camera (Coolview; Photonic Science Ltd.) and grabber software (ImageAccess V2.04K; Imagic Bildverarbeitung AG). Western blot analysis with E-cadherin or anti-αSMA or with anti-pMLC antibodies was performed as described above.

Results

RCC express a novel mb-IL-15 independent of IL-15R. We and others have previously shown that RCC do no secrete detectable amount of free IL-15 (23, 28) but express a mb-IL-15 not anchored through the IL-15Rα chain (24). We, here, further investigate the properties of IL-15 in RCC. In Fig. 1*A*, flow cytometry shows that different RCC express a mb-IL-15, whose intensity is not decreased by acidic treatment that, in contrast, causes the disappearance of mb-IL-15 in UT7 erythroleukemic cells known to transpresent IL-15 through the IL-15Rα chain (28). In addition, treatment with the phosphorylated lipase C causes a significant decrease in the membrane expression of the glycosylphosphatidylinositol

Published OnlineFirst February 3, 2009; DOI: 10.1158/0008-5472.CAN-08-3198

(GPI)-anchored CD59 protein, whereas mb-IL-15 expression in RCC7 is not affected, suggesting that mb-IL-15 is not a GPI-linked protein (19).

Reverse transcription–PCR (RT-PCR) analysis strengthens flow cytometry data showing that RCC cell lines (HIEG and ACHN), primary cultures of healthy renal tissue, primary tumor and metastasis derived from the same patient (RCC5-N, RCC5-T, RCC5-Met), and primary tumor RCC7 cells and virus transformed epithelial embryonic kidney cells (HK2) only express the 536 transcript coding for the secretable IL-15 form (29). In addition, RCC do not express the transcript for the γc chain (Fig. 1*B*), whereas the IL-15Rα and β subunits are detected on their surface (Supplementary Fig. S1).

In Fig. 1*C*, mb-IL-15 from RCC7 cells was analyzed by Western blotting using the L-20 antibody. Data show that RCC7 cells express a specific band at 27 kDa, whereas the "canonical" monomeric 14-kDa IL-15 band was only detected in lipopolysaccharide-treated human monocytes. In addition, L-20 antibody recognizes the rhIL-15 monomeric form starting from the concentrations of 0.1 to 0.5 μg/mL, whereas the use of increasing concentrations of rhIL-15 causes the appearance of a specific 27-kDa band.

To strengthen the above data, membrane fractions from three different RCC (RCC7, HIEG, and HK2) were immunoprecipitated and blotted with the anti-IL-15 antibody L-20 (Fig. 1*D*). This led to the detection of a single specific band of 27 kDa in the three cell lines tested.

Overall, the data presented in Fig. 1 indicate that RCC express the IL-15 protein predominantly as a 27-kDa putative homodimeric membrane-bound form, which is anchored at the cell membrane in an IL-15R and GPI-independent manner.

RCC express a mb-IL-15 sensitive to matrix metalloproteinases. It has been reported that the shedding of mb-IL-15Rα as a soluble

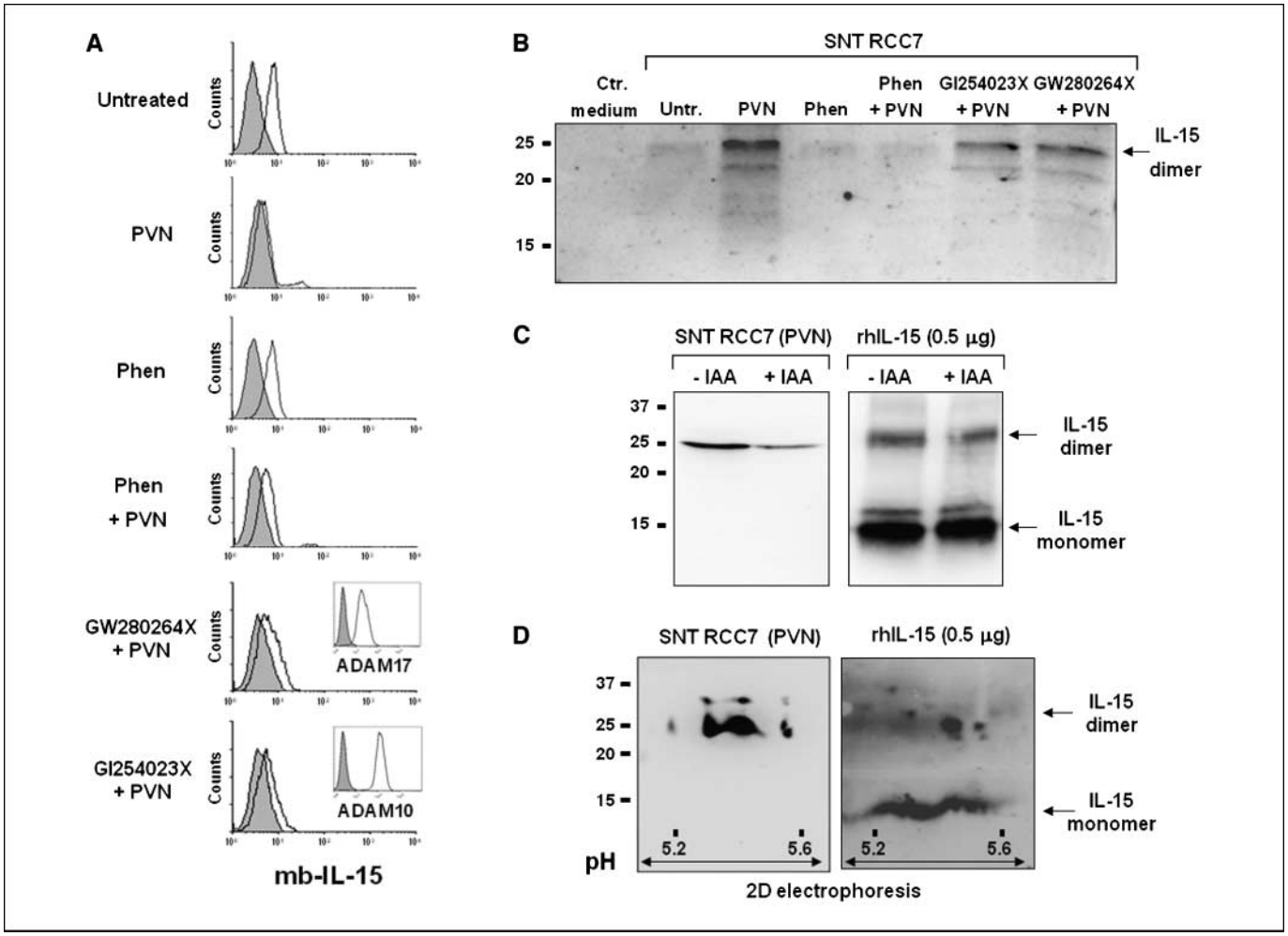

Figure 2. Sensitivity to MMPs of mb-IL-15 on human RCC. *A,* flow cytometric analysis of mb-IL-15 expression (mAb 247-PE, *open peaks*) on human RCC7 cells before and after 3 h of treatment with PVN (200 μmol/L) in the presence or not of the broad spectrum MMP inhibitor Phen (2 mmol/L) and 10 μmol/L specific inhibitors for ADAM17 (*GW280264X*) and ADAM10 (*GI254023X*). *Inset,* flow cytometric analysis of ADAM10 and ADAM17 membrane expression in RCC (*open peaks*). Isotype-matched antibodies were used as control (*shaded peaks*). These data are representative of three independent experiments. *B,* Western blot analysis with anti-IL-15 antibody L-20 on the concentrated supernatant (*SNT*) of RCC7 cells treated or not (*Untr.*) for 3 h with PVN in the presence or not of broad spectrum (*Phen*) and specific GW280264X and GI254023X MMPs inhibitors. Fresh medium was used as control (*Ctr. medium*). Representative of three different experiments. *C,* comparison by Western blot analysis with anti-IL-15 antibody L-20, under stringent reducing and denaturing conditions in the presence or not of iodoacetamide (100 mmol/L), of the concentrated supernatant of RCC7 cells treated for 3 h with PVN and the rhIL-15 at 0.5 μg. Representative of three different experiments. *D,* bidimensional electrophoretic profile of IL-15 in serum-free RCC7 concentrated cell medium after PVN treatment or in 0.5 μg of rhIL-15. Immobiline DryStrips were rehydrated with 200 μL each and analyzed by two-dimensional electrophoresis on a 3-11 NL pH gradient strip for the first dimension and then by SDS-PAGE for the second dimension and immunoblotted with anti-IL-15 antibody L-20.

Published OnlineFirst February 3, 2009; DOI: 10.1158/0008-5472.CAN-08-3198

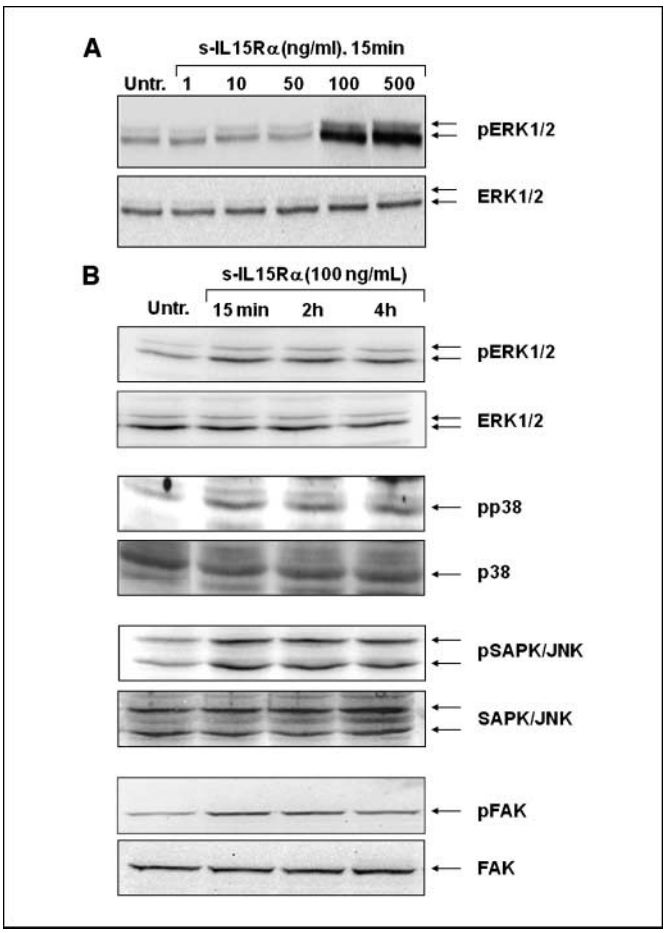

Figure 3. Induction of mb-IL-15–dependent reverse signal. *A,* Western blot analysis of MAPK ERK1/2 activation, using an anti-pERK1/2 antibody after 15-min treatment of RCC7 with increasing concentrations (1–500 ng/mL) of s-IL-15Rα chain. *B,* time course Western blot analysis of MAPK ERK1/2, p38, SAPK/JNK, and FAK activation in confluent RCC cells stimulated with 100 ng/mL of s-IL-15Rα chain. Membranes were reblotted with ERK1/2, p38, SAPK/JNK, and FAK antibodies used as loading controls. Representative of three independent experiments.

receptor is controlled by ADAM17 (14) and possibly by other matrix metalloproteinases (MMP), but there is no evidence that such a mechanism may concern the mb-IL-15 forms. Flow cytometric analysis in Fig. 2*A* shows that mb-IL-15 expressed by RCC7 is cleaved and shed after 3 hours of treatment with PVN, a potent activator of MMPs (30). The mb-IL-15 shedding induced by PVN is blocked either in the presence of a large spectrum MMP inhibitor, such as Phen, or specific competitors of ADAM17 (GW280264X) and ADAM10 (GI254023X), indicating therefore that different MMPs may control the shedding of mb-IL-15. The specificity of the effects mediated by the competitors for ADAM10 and ADAM17 was assessed by flow cytometry showing that RCC7 cells express detectable amounts of ADAM10 and ADAM17 (Fig. 2*A, inset*). Similar results were observed studying HIEG and HK2 cell lines, and the above-mentioned treatments had no toxic effects on RCC (Supplementary Fig. S2).

Subsequently, we extended the flow cytometry data, analyzing by Western blot the supernatants of RCC7 cells before and after 3 hours of PVN treatment (Fig. 2*B*). In concentrated supernatants of PVN-treated RCC7, a single band of ~25 kDa was detected, using the anti-IL-15 L-20 antibody. This IL-15–specific band is totally (Phen) or partially (ADAM10 and ADAM17 inhibitors) inhibited in supernatants of cells treated with PVN.

IL-2 spontaneously forms noncovalent and covalent self-associations (31); thereby, we investigated whether the IL-15 homodimers detected in rhIL-15 and putative mb-IL-15 homodimers released by PVN-treated RCC were generated through SH2 bridges, incubating both samples with iodoacetamide. Western blot analysis performed in stringent reducing and denaturing conditions shows that iodoacetamide treatment (Fig. 2*C*) does not modify the migratory pattern of both IL-15, suggesting that their covalent dimerization is not due to SH2 bridges. Further characterization by two-dimensional electrophoresis shows that both samples display similar charges at distributions between pH 5.2 and 5.6 without differences in their original molecular weight (Fig. 2*D*).

In human RCC, s-IL-15Rα chain triggers mb-IL-15–dependent reverse signaling. It has been reported that a mb-IL-15 constitutively expressed by PC-3 human prostate carcinoma cells (PCC) is involved in reverse signaling activation upon stimulation with low concentrations (1 ng/mL) of s-IL-15Rα (8).

We have recently shown that the mb-IL-15 form expressed by RCC7 is functional and triggers signaling in NK cells (24). We further investigate if mb-IL-15 is able to induce reverse signaling upon stimulation with specific soluble ligands in RCC. We show a significant increase of ERK1/2 phosphorylation in RCC7 cells treated with at least 100 ng/mL of s-IL-15Rα (Fig. 3*A*). In addition, time course experiments with 100 ng/mL of s-IL-15Rα chain show that, in RCC7 cells, there is a rapid and significant increase of mitogen-activated protein kinase (MAPK; pERK1/2, p38, pSAPK/JNK) and FAK phosphorylation (Fig. 3*B*).

mb-IL-15–dependent reverse signaling induces EMT of RCC. The coordinated activation of the ERK1/2 and FAK pathways promotes early changes in the dynamic reorganization of the cytoskeleton controlling α-SMA polymerization, focal adhesion dynamics, and down-regulation of E-cadherin protein levels in several cell systems (32, 33). On the other hand, activation of p38 MAPK and/or JNK pathways results in an increased α-SMA expression and physiologic regulation of intermediate filaments (34, 35).

Thus, we investigated the effects of mb-IL-15 stimulation with the s-IL-15Rα chain on the morphology and cytoskeleton reorganization of RCC. Figure 4*A* shows that untreated control RCC7 cells display an epithelial-like morphology, confirmed by the expression of E-cadherin and ZO-1 (two major epithelial markers) and the absence of a detectable α-SMA and vimentin networks. Remarkably, RCC7, after 6 days of treatment with 5 ng/mL of TGF-β or with 100 ng/mL of s-IL-15Rα chain, lose E-cadherin and ZO-1 expression and acquire a mesenchymal morphology associated to a cytoskeletal reorganization characterized by the formation of strong α-SMA stress fibers and a diffuse vimentin network. In addition, decreased levels of E-cadherin associated to a significant increase in α-SMA synthesis and phosphorylation of the myosin light chain (MLC; a major marker of the contractile function) were detected by Western blotting (Fig. 4*B*), confirming immunofluorescence analyses.

Altogether, these results show that the stimulation of mb-IL-15 with s-IL-15Rα chain triggers, in RCC, EMT, illustrating a novel powerful protumoral property of IL-15.

mb-IL-15–dependent reverse signal is hindered by a specific control mechanism. In human PC-3 PCC and human monocytes,

Published OnlineFirst February 3, 2009; DOI: 10.1158/0008-5472.CAN-08-3198

1 ng/mL of s-IL-15Rα chain is sufficient to induce the reverse signal (8), whereas in RCC, the minimal concentration of s-IL-15Rα is 100 ng/mL. PC-3 cells, in contrast to RCC, do not express IL-15R. Thus, in RCC, mb-IL-15 interacting with IL-15Rα, on the surface of the same cell, could compete with low concentrations of s-IL-15Rα chain for mb-IL-15 binding, preventing a reverse signal. In this context, induction of a reverse signal may require much higher concentrations of the soluble ligand.

The existence of IL-15/IL-15Rα complexes is shown by immunoprecipitation experiments. Whereas IL-15 immunoprecipitated from RCC7 cells (using the L-20 antibody) and blotted using the same antibody reveals a single specific 27-kDa band, the immunoprecipitation of IL-15 membrane, reblotted with the anti-IL-15Rα mAb 147, shows a specific band of ~50 kDa (Fig. 5*A*). To assess if the association of IL-15Rα chain with mb-IL-15 in RCC7 was able to interfere on reverse signal activation using low concentrations of the s-IL-15Rα chain (1–10 ng/mL), we tried to dissociate the IL-15Rα chain from the cell surface by short acidic treatment (pH 4.0). IL-15Rα chain is detected at the surface of human monocytes and RCC7 cells (Fig. 5*B*). In monocytes, the IL-15Rα chain is strongly expressed and is resistant to acidic shock. In contrast, in RCC7 cells, the IL-15Rα chain is highly sensitive to the acid buffer and totally dissociated from the cell membrane. These data suggest that the IL-15Rα chain, depending on the cell type, may be found in different compartments, which are defined on the basis of a differential sensitivity to acidic shock. Subsequently, acidic treated and untreated RCC7 cells were stimulated 3 hours later with increasing concentrations of s-IL-15Rα (1–100 ng/mL) for 15 minutes and analyzed by Western blot for the phosphorylation of MAPK ERK1/2 (Fig. 5*C*). Transient removal of IL-15Rα chain resulted in increased ERK1/2 phosphorylation in response to low concentrations of s-IL-15Rα (1–10 ng/mL), whereas in untreated RCC7 cells, ERK1/2 phosphorylation required stimulation with 100 ng/mL of s-IL-15Rα. Similar results were obtained using the silencing of the IL-15Rα gene by specific small interfering RNAs (Supplementary Fig. S3) fully supporting the initial hypothesis.

Discussion

This study reports that human RCC constitutively express a novel form of mb-IL-15, which, in response to soluble specific ligands such as s-IL-15Rα chain, triggers a complex reverse signaling leading to the development of EMT, a property that favors tumor invasiveness (36, 37). In addition, RCC secrete two s-IL-15Rα isoforms of 35 and 40 kDa, creating the possibility of a continuous functional cross-talk with mb-IL-15 to modify the properties of the tumor cells themselves and/or the behavior of the infiltrated immune cells.

Human RCC constitutively express a mb-IL-15 not dependent on the expression of the trimeric IL-15R complex (13, 17, 18, 20). Indeed, short treatment with an acidic buffer (pH 4.0) does not modify mb-IL-15 present in RCC. In addition, RCC do not express the γc chain. Therefore, mb-IL-15 expressed by RCC has the characteristics of the "so-called" transmembrane-anchored IL-15 constitutively expressed on the cell surface of human PCC. However, two major features distinguish RCC mb-IL-15 from the PCC/monocyte mb-IL-15 form: (*a*) its molecular weight is 27 kDa and (*b*) its shedding is a 25-kDa protein induced by enzymatic cleavage operated by ADAM10 and ADAM17 metalloproteases. Natural PCC/monocyte mb-IL-15 form and recombinant IL-15 display a molecular weight of 13.5 to 14 kDa (1, 14), whereas the RCC mb-IL-15 form is detected by Western blot and immunoprecipitation as a band of 27 kDa. These results are obtained using the anti-IL-15 polyclonal IgG L-20, which does not detect in RCC lysates the traditional 13.5-kDa to 14-kDa band, whereas it recognizes this form in lipopolysaccharide-treated monocyte lysates or when using the recombinant cytokine at concentrations ranging between 0.5 and 3 μg/mL. These data strongly suggest that the 14-kDa IL-15 form is not or too faintly expressed by RCC. Because it has been recently proposed that free IL-15 is highly prone to self-aggregation (38), similar to what was previously observed for IL-2 (31), the most likely explanation is that the 27-kDa band represents a homodimer that seems to be the predominant form of IL-15 expressed by RCC. This conclusion is also strengthened by the comparison of the biochemical properties exhibited by the "true" homodimers detected in rhIL-15 samples and the "putative" IL-15 homodimers found in RCC. Indeed, monodimensional and bidimensional electrophoretic analyses performed under stringent reducing and denaturing conditions in

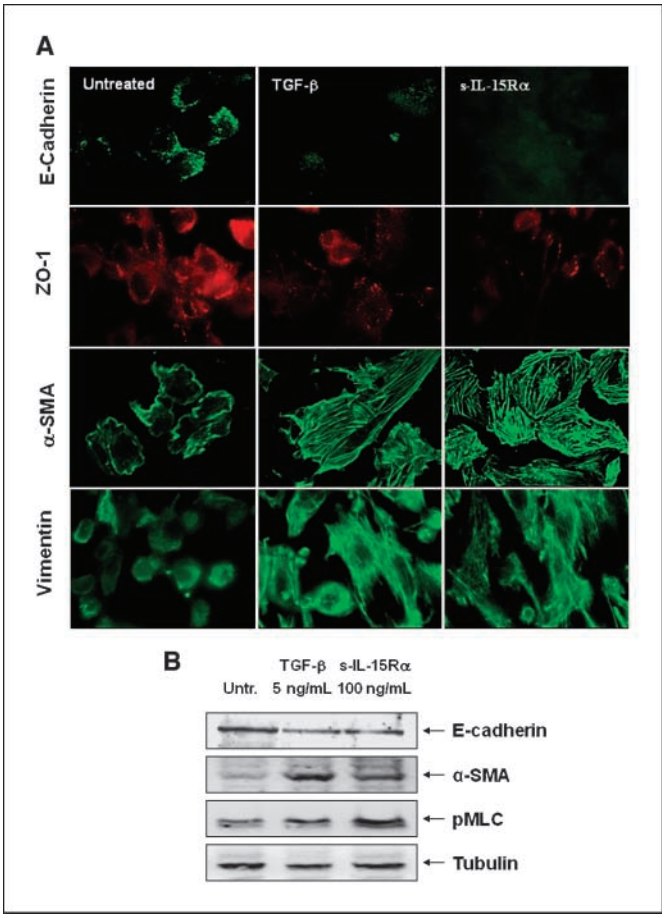

Figure 4. mb-IL-15 can function as a receptor to induce EMT in confluent RCC. *A,* analysis by immunocytochemistry in 6-d-old (*d6*) RCC cultures of expression of the epithelial markers E-cadherin and ZO-1 and of the mesenchymal markers α-SMA and vimentin. *Left,* untreated RCC7; *middle,* RCC7 stimulated with 5 ng/mL of TGF-β; *right,* RCC7 stimulated with 100 ng/mL of s-IL-15Rα chain. Representative of three different experiments. *B,* Western blot analysis of E-cadherin, α-SMA expression, and pMLC activation in 6-d-old (*d6*) RCC cultures stimulated with 100 ng/mL of s-IL-15Rα chain or with 5 ng/mL of TGF-β. Membranes were rebottled with anti-α-tubulin antibody to check load charge control. Representative of three different experiments.

Published OnlineFirst February 3, 2009; DOI: 10.1158/0008-5472.CAN-08-3198

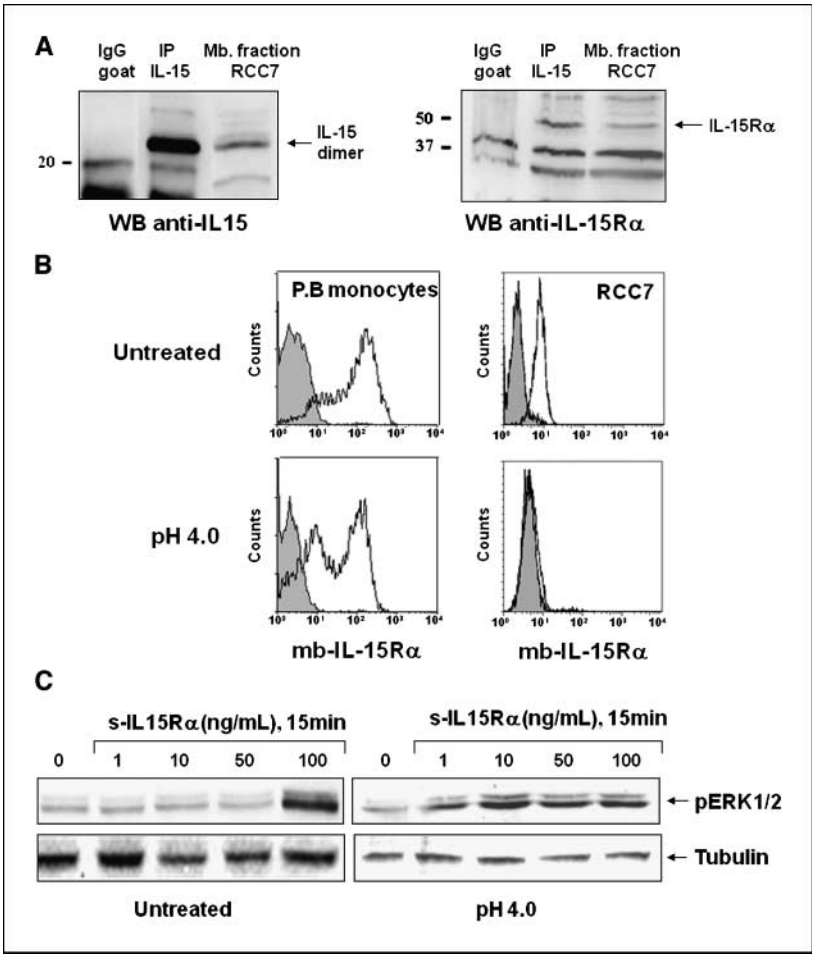

Figure 5. mb-IL-15–dependent reverse signal is locked by a *cis* association with membrane-associated IL-15Rα subunit. *A,* coimmunoprecipitation with an anti-IL-15 goat antibody L-20 on membrane fraction (*Mb. fraction*) of RCC7 cell line. The immunoprecipitation membrane was probed by Western blotting with the same L-20 antibody. A single 27-kDa specific band was detected. The same membrane was subsequently reprobed with anti-IL-15Rα mAb 147. A specific band of ~50 kDa was detected. No bands were detected with isotype controls (goat IgG). Representative of three different experiments. *B,* flow cytometry analysis of IL-15Rα membrane expression (mb-IL-15Rα, *open peaks*) in human peripheral blood monocytes (used as positive control) and in RCC7 cells treated or not with acidic buffer (pH 4.0 at 4°C for 15 min). Isotype-matched antibodies were used as control (*shaded peaks*). Representative of three different experiments. *C,* Western blot analysis of MAPK ERK1/2 phosphorylation in RCC7 cells. RCC cultures were stimulated or not for 15 min with increasing concentrations (1–100 ng/mL) of recombinant s-IL-15Rα added 3 h after acidic shock. PVDF membranes were reblotted with antitubulin antibody to check load charge control. Rrepresentative of three different experiments.

the presence of iodoacetamide show that the recombinant and the natural IL-15 27-kDa bands share several similarities, suggesting a covalent homodimeric nature whose self-aggregation is not due to SH2 bridges.

On the other hand, in RCC, the enzymatic shedding of mb-IL-15 homodimeric form of 25 kDa is an original property that opens interesting perspectives. Indeed, the "shed mb-IL-15" interacting with the natural s-IL-15Rα chain codetected in the supernatant of PMA-treated RCC forms a s-IL-15 (25 kDa)/IL-15Rα (35 kDa) complex (Supplementary Fig. S4) that could exert either agonist or antagonist effects. Indeed, similar complexes (hyper IL-15) formed in the tumor microenvironment could acquire the competence to stimulate lymphoid cells bearing the low-affinity IL-15R (17). Alternatively, the shed homodimer could act as a decoy molecule for the s-IL-15Rα. In both situations, the intratumoral immune response would be heavily modified. In addition, because the natural s-IL-15Rα forms a complex with the shed IL-15 homodimer, we propose that it could also recognize the mb-IL-15 homodimer and deliver a reverse signal in RCC.

Similar to what was previously reported for the PCC/monocyte mb-IL-15 form, the mb-IL-15 expressed by RCC is also competent for delivering a bidirectional signal. Indeed, RCC mb-IL-15 protects from apoptosis NK cells through transpresentation mechanism (24) and, in addition, triggers reverse signaling upon stimulation with s-IL-15Rα, mediating outside-to-inside signal transduction. Thus, we observed that stimulation with the s-IL-15Rα chain induces the phosphorylation of several MAPKs (ERK1/2, p38, SAPK/JNK) and FAK. The major biological effect consequent to the reverse signal is the induction of EMT. EMT is a major biological event that, in carcinoma cells, leads to the acquisition of an increased motility and, therefore, of metastatic potential and is essentially mediated by Oncostatin M, TGF-β, and/or CTGF (39, 40). EMT is a complex, highly regulated process that involves the development of migratory/contractile properties (acquisition of a mesenchymal phenotype; ref. 32) associated to the loss and/or redistribution of the epithelial markers E-cadherin and ZO-1, which are essential steps for the accomplishment of EMT and the development of tumorigenesis (41). During this process, activated ERK and FAK are upstream regulators of specific machineries that affect the formation of focal adhesions through the phosphorylation of MLC, dynamic reorganization of the actin cytoskeleton with the formation of enhanced tensile stress fibers (42, 43), whereas synthesis of α-SMA and organization of the intermediate filament network seem to be under the control of the p38 and SAPK/JNK pathways (44, 45). On the other hand, decreased E-cadherin expression is controlled by ERK1/2 and p38 (46), whereas down-regulation of ZO-1 expression seems to be uniquely controlled by ERK1/2 activation (47). In human kidney, promotion and

Published OnlineFirst February 3, 2009; DOI: 10.1158/0008-5472.CAN-08-3198

development of EMT is based on interactions between different inflammatory factors and resident tubular epithelial cells (48–50). Herein, we show that, in RCC, stimulation of mb-IL-15 with the soluble specific ligand s-IL-15Rα is necessary and sufficient to trigger all the above-mentioned biochemical events and to induce efficient EMT, illustrating that mb-IL-15 interactions with the s-IL-15Rα chain may lead to the development of a wide spectrum of protumoral activities, which depend on the cell system explored (8, 9).

Previous papers have shown that the secretion of free IL-15 is drastically controlled at both transcriptional and posttranscriptional levels, likely for limiting the availability and possibly the effects of this powerful proinflammatory factor (1). In contrast, the existence of control mechanisms that modulate the expression/function of mb-IL-15 has not yet been reported. In this context, we describe a third variable that distinguishes the mb-IL-15 form expressed by RCC from that detected in PCC and human monocytes. Indeed, in former ones, it is necessary to use a 100-fold higher concentration of the s-IL-15Rα chain to trigger the reverse signal. Our data indicate that the most likely explanation is that RCC express at their surface the IL-15Rα chain, whereas PCC do not express IL-15R (8) and human monocytes do not express the acidic shock-sensitive IL-15Rα detected in RCC. In these conditions, in RCC, mb-IL-15 interacts *in cis* with neighboring acidic shock-sensitive IL-15Rα that lock the specific epitope on mb-IL-15, competing successfully with the soluble receptor delivered at a low concentration (1 ng/mL).

In conclusion, hijacking of the IL-15/IL-15R system for promoting tumor survival and escape from host defenses is a property displayed by several human cancer cells. However, each tumor develops strategies adapted to its specific cellular environment. Indeed, whereas bronchial and colon cancer cells secrete IL-15 that, acting through classic autocrine/paracrine loops, develop proinflammatory and proangiogenic properties (9, 51), melanoma cells display both IL-15 secretion and IL-15 nuclear localization, favoring tumor escape mechanisms (7, 11). On the other hand, in head and neck carcinoma, there is a correlation between secretion of the IL-15Rα chain and poor clinical outcome. In this model, the soluble receptor, interacting with IL-15 secreted by environmental cells, triggers proinflammatory effects (44). Finally, PCC and RCC express mb-IL-15 forms competent for delivering bidirectional signaling and responsible for the induction of protumoral properties (8, 24). Nevertheless, four major differences distinguish the mb-IL-15 form expressed by RCC: (*a*) its expression as a functional homodimer, (*b*) its metalloprotease-dependent shedding in the tumor microenvironment, (*c*) the induction of EMT, and (*d*) the existence of a control mechanism, represented by the interaction *in cis* with membrane-associated IL-15Rα chain that competes with the soluble counterparts regulating the induction of reverse signals. This particular IL-15/IL-15Rα hindering interplay could represent a conversion mechanism that favors the trans-presentation functions. Alternatively, it could constitute a defense mechanism to avoid continuous activation of reverse signals by the s-IL-15Rα chain secreted in the intratumoral microenvironment by the tumor cells themselves or by other cellular sources.

We cannot exclude that the peculiar mb-IL-15/IL-15Rα interactions herewith reported in RCC may be shared by other tumor cells. However, it must be stated that renal cancers seem to be much more efficient than other tumors because they associate genetic mechanisms leading to constitutive HIF activation (52) to the secretion of immunosuppressive molecules (53) and to hijacking of the IL-15/IL-15R system, which favors tumor invasiveness.

Disclosure of Potential Conflicts of Interest

The authors state that there is no conflict of interest.

Acknowledgments

Received 8/19/2008; revised 11/4/2008; accepted 11/6/2008; published OnlineFirst 02/03/2009.

Grant support: Agence Française de Biomedicine, ARC grant 3143, InCa, Associazione Italiana per la Ricerca sul Cancro, and Italian Ministry of Health. K. Khawam was recipient of fellowships by Centre National de la Recherche Scientifique-Libanais, NRB-Vaincre le Cancer, and Société Française de Néphrologie. Y. Gu was recipient of an NRB-Vaincre le Cancer postdoctoral fellowship. M. Giuliani was recipient of a FNAIR postdoctoral fellowship.

The costs of publication of this article were defrayed in part by the payment of page charges. This article must therefore be hereby marked *advertisement* in accordance with 18 U.S.C. Section 1734 solely to indicate this fact.

References

1. Waldmann TA. The biology of interleukin-2 and interleukin-15: implications for cancer therapy and vaccine design. Nat Rev Immunol 2006;6:595–601.
2. Teague RM, Sather BD, Sacks JA, et al. Interleukin-15 rescues tolerant CD8+ T cells for use in adoptive immunotherapy of established tumors. Nat Med 2006;12:335–41.
3. Kobayashi H, Dubois S, Sato N, et al. Role of trans-cellular IL-15 presentation in the activation of NK cell-mediated killing, which leads to enhanced tumor immunosurveillance. Blood 2005;105:721–7.
4. Yajima T, Nishimura H, Wajjwalku W, Harada M, Kuwano H, Yoshikai Y. Overexpression of interleukin-15 *in vivo* enhances antitumor activity against MHC class I-negative and -positive malignant melanoma through augmented NK activity and cytotoxic T-cell response. Int J Cancer 2002;99:573–8.
5. Seike M, Yanaihara N, Bowman ED, et al. Use of a cytokine gene expression signature in lung adenocarcinoma and the surrounding tissue as a prognostic classifier. J Natl Cancer Inst 2007;99:1257–69.
6. Allen C, Duffy S, Teknos T, et al. Nuclear factor-κB-related serum factors as longitudinal biomarkers of response and survival in advanced oropharyngeal carcinoma. Clin Cancer Res 2007;13:3182–90.
7. Barzegar C, Meazza R, Pereno R, et al. IL-15 is produced by a subset of human melanomas, and is involved in the regulation of markers of melanoma progression through juxtacrine loops. Oncogene 1998;16:2503–12.
8. Budagian V, Bulanova E, Orinska Z, et al. Reverse signaling through membrane-bound interleukin-15. J Biol Chem 2004;279:42192–201.
9. Kuniyasu H, Ohmori H, Sasaki T, et al. Production of interleukin 15 by human colon cancer cells is associated with induction of mucosal hyperplasia, angiogenesis, and metastasis. Clin Cancer Res 2003;9:4802–10.
10. Nguyen ST, Hasegawa S, Tsuda H, et al. Identification of a predictive gene expression signature of cervical lymph node metastasis in oral squamous cell carcinoma. Cancer Sci 2007;98:740–6.
11. Pereno R, Giron-Michel J, Gaggero A, et al. IL-15/IL-15Rα intracellular trafficking in human melanoma cells and signal transduction through the IL-15Rα. Oncogene 2000;19:5153–62.
12. Sasahira T, Sasaki T, Kuniyasu H. Interleukin-15 and transforming growth factor α are associated with depletion of tumor-associated macrophages in colon cancer. J Exp Clin Cancer Res 2005;24:69–74.
13. Budagian V, Bulanova E, Paus R, Bulfone-Paus S. IL-15/IL-15 receptor biology: a guided tour through an expanding universe. Cytokine Growth Factor Rev 2006;17:259–80.
14. Budagian V, Bulanova E, Orinska Z, et al. Natural soluble interleukin-15Rα is generated by cleavage that involves the tumor necrosis factor-α-converting enzyme (TACE/ADAM17). J Biol Chem 2004;279:40368–75.
15. Bulanova E, Budagian V, Duitman E, et al. Soluble Interleukin IL-15Rα is generated by alternative splicing or proteolytic cleavage and forms functional complexes with IL-15. J Biol Chem 2007;282:13167–79.
16. Mortier E, Bernard J, Plet A, Jacques Y. Natural, proteolytic release of a soluble form of human IL-15 receptor α-chain that behaves as a specific, high affinity IL-15 antagonist. J Immunol 2004;173:1681–8.

17. Giron-Michel J, Giuliani M, Fogli M, et al. Membrane-bound and soluble IL-15/IL-15Rα complexes display differential signaling and functions on human hematopoietic progenitors. Blood 2005;106:2302–10.

18. Mortier E, Quemener A, Vusio P, et al. Soluble interleukin-15 receptor α (IL-15Rα)-sushi as a selective and potent agonist of IL-15 action through IL-15Rβ/γ. Hyperagonist IL-15 x IL-15R α fusion proteins. J Biol Chem 2006;281:1612–9.

19. Bulfone-Paus S, Bulanova E, Budagian V, Paus R. The interleukin-15/interleukin-15 receptor system as a model for juxtacrine and reverse signaling. BioEssays 2006;28:362–77.

20. Dubois S, Mariner J, Waldmann TA, Tagaya Y. IL-15Rα recycles and presents IL-15 In trans to neighboring cells. Immunity 2002;17:537–47.

21. Pavlakis M, Strehlau J, Lipman M, Shapiro M, Maslinski W, Strom TB. Intragraft IL-15 transcripts are increased in human renal allograft rejection. Transplantation 1996;62:543–5.

22. Shinozaki M, Hirahashi J, Lebedeva T, et al. IL-15, a survival factor for kidney epithelial cells, counteracts apoptosis and inflammation during nephritis. J Clin Invest 2002;109:951–60.

23. Trinder P, Seitzer U, Gerdes J, Seliger B, Maeurer M. Constitutive and IFN-γ regulated expression of IL-7 and IL-15 in human renal cell cancer. Int J Oncol 1999; 14:23–31.

24. Wittnebel S, Da Rocha S, Giron-Michel J, et al. Membrane-bound interleukin (IL)-15 on renal tumor cells rescues natural killer cells from IL-2 starvation-induced apoptosis. Cancer Res 2007;67:5594–9.

25. Viey E, Fromont G, Escudier B, et al. Phosphostim-activated γ δ T cells kill autologous metastatic renal cell carcinoma. J Immunol 2005;174:1338–47.

26. Hundhausen C, Misztela D, Berkhout TA, et al. The disintegrin-like metalloproteinase ADAM10 is involved in constitutive cleavage of CX3CL1 (fractalkine) and regulates CX3CL1-mediated cell-cell adhesion. Blood 2003;102:1186–95.

27. Giron-Michel J, Fogli M, Gaggero A, et al. Detection of a functional hybrid receptor γc/GM-CSFRβ in human hematopoietic CD34+ cells. J Exp Med 2003;197:763–75.

28. Giuliani M, Giron-Michel J, Negrini S, et al. Generation of a novel regulatory NK cell subset from peripheral blood CD34+ progenitors promoted by membrane-bound IL-15. PLoS ONE 2008;3:e2241.

29. Gaggero A, Azzarone B, Andrei C, et al. Differential intracellular trafficking, secretion and endosomal localization of two IL-15 isoforms. Eur J Immunol 1999;29: 1265–74.

30. Vecchi M, Rudolph-Owen LA, Brown CL, Dempsey PJ, Carpenter G. Tyrosine phosphorylation and proteolysis. Pervanadate-induced, metalloprotease-dependent cleavage of the ErbB-4 receptor and amphiregulin. J Biol Chem 1998;273:20589–95.

31. Kaplan DR. Delivery of interleukin 2 for immunotherapy. J Chromatogr B Biomed Appl 1994;662:315–23.

32. Flanders KC. Smad3 as a mediator of the fibrotic response. Int J Exp Pathol 2004;85:47–64.

33. Schober M, Raghavan S, Nikolova M, et al. Focal adhesion kinase modulates tension signaling to control actin and focal adhesion dynamics. J Cell Biol 2007;176: 667–80.

34. Cheng TJ, Lai YK. Identification of mitogen-activated protein kinase-activated protein kinase-2 as a vimentin kinase activated by okadaic acid in 9L rat brain tumor cells. J Cell Biochem 1998;71:169–81.

35. Vepachedu R, Gorska MM, Singhania N, Cosgrove GP, Brown KK, Alam R. Unc119 regulates myofibroblast differentiation through the activation of Fyn and the p38 MAPK pathway. J Immunol 2007;179:682–90.

36. Guarino M, Rubino B, Ballabio G. The role of epithelial-mesenchymal transition in cancer pathology. Pathology 2007;39:305–18.

37. Hugo H, Ackland ML, Blick T, et al. Epithelial-mesenchymal and mesenchymal-epithelial transitions in carcinoma progression. J Cell Physiol 2007;213:374–83.

38. Olsen SK, Ota N, Kishishita S, et al. Crystal structure of the interleukin-15 receptor α complex: insights into trans and cis presentation. J Biol Chem 2007;282:37191–204.

39. Gore-Hyer E, Shegogue D, Markiewicz M, et al. TGF-β and CTGF have overlapping and distinct fibrogenic effects on human renal cells. Am J Physiol Renal Physiol 2002;283:F707–16.

40. Nightingale J, Patel S, Suzuki N, et al. Oncostatin M, a cytokine released by activated mononuclear cells, induces epithelial cell-myofibroblast transdifferentiation via Jak/Stat pathway activation. J Am Soc Nephrol 2004; 15:21–32.

41. Carothers AM, Javid SH, Moran AE, Hunt DH, Redston M, Bertagnolli MM. Deficient E-cadherin adhesion in C57BL/6J-Min/+ mice is associated with increased tyrosine kinase activity and RhoA-dependent actomyosin contractility. Exp Cell Res 2006;312:387–400.

42. Hong T, Grabel LB. Migration of F9 parietal endoderm cells is regulated by the ERK pathway. J Cell Biochem 2006;97:1339–49.

43. Webb DJ, Donais K, Whitmore LA, et al. FAK-Src signaling through paxillin, ERK and MLCK regulates adhesion disassembly. Nat Cell Biol 2004;6:154–61.

44. Badoual C, Bouchaud G, Agueznay Nel H, et al. The soluble α chain of interleukin-15 receptor: a proinflammatory molecule associated with tumor progression in head and neck cancer. Cancer Res 2008;68:3907–14.

45. Zhang M, Tang J, Li X. Interleukin-1β-induced transdifferentiation of renal proximal tubular cells is mediated by activation of JNK and p38 MAPK. Nephron Exp Nephrol 2005;99:e68–76.

46. Li M, Hering-Smith KS, Simon EE, Batuman V. Myeloma light chains induce epithelial-mesenchymal transition in human renal proximal tubule epithelial cells. Nephrol Dial Transplant 2008;23:860–70.

47. Wang Y, Zhang J, Yi XJ, Yu FS. Activation of ERK1/2 MAP kinase pathway induces tight junction disruption in human corneal epithelial cells. Exp Eye Res 2004;78: 125–36.

48. Burns WC, Kantharidis P, Thomas MC. The role of tubular epithelial-mesenchymal transition in progressive kidney disease. Cells Tissues Organs 2007;185:222–31.

49. Liu Y. Epithelial to mesenchymal transition in renal fibrogenesis: pathologic significance, molecular mechanism, and therapeutic intervention. J Am Soc Nephrol 2004;15:1–12.

50. Wahab NA, Mason RM. A critical look at growth factors and epithelial-to-mesenchymal transition in the adult kidney. Interrelationships between growth factors that regulate EMT in the adult kidney. Nephron Exp Nephrol 2006;104:e129–34.

51. Ge N, Nishioka Y, Nakamura Y, et al. Synthesis and secretion of interleukin-15 by freshly isolated human bronchial epithelial cells. Int Arch Allergy Immunol 2004;135:235–42.

52. Rathmell WK, Chen S. VHL inactivation in renal cell carcinoma: implications for diagnosis, prognosis and treatment. Expert Rev Anticancer Ther 2008;8:63–73.

53. Seliger B, Schlaf G. Structure, expression and function of HLA-G in renal cell carcinoma. Semin Cancer Biol 2007;17:444–50.

Cancer Research
The Journal of Cancer Research (1916–1930) | The American Journal of Cancer (1931–1940)

AACR American Association for Cancer Research

Human Renal Cancer Cells Express a Novel Membrane-Bound Interleukin-15 that Induces, in Response to the Soluble Interleukin-15 Receptor α Chain, Epithelial-to-Mesenchymal Transition

Krystel Khawam, Julien Giron-Michel, Yanhong Gu, et al.

Cancer Res 2009;69:1561-1569. Published OnlineFirst February 3, 2009.